

machinery. Interestingly, delayed removal of either mutant or slightly different wild-type paternal mitochondria results in increased embryonic lethality in heteroplasmic animals, likely due to incompatibility in cellular signaling between the mitochondrial and nuclear genomes (15, 17). This provides evidence that persistence of paternal mitochondria compromises animal development and may be the impetus for maternal inheritance of mitochondria. DeLuca and O'Farrell showed that endonuclease G mediated the degradation of sperm mitochondrial DNA during *Drosophila* spermatogenesis before fertilization and hypothesized that this degradation helped prevent paternal mtDNA transmission (21). In contrast, we find in *C. elegans* that CPS-6 acts after fertilization to mediate degradation of both paternal mitochondria and mtDNA to facilitate their autophagic degradation. These findings imply a conserved role of endonuclease G in paternal mtDNA elimination and expand the roles of this nuclease beyond apoptosis and mitochondrial maintenance (8, 9, 22).

## REFERENCES AND NOTES

1. S. E. Calvo, V. K. Mootha, *Annu. Rev. Genomics Hum. Genet.* **11**, 25–44 (2010).
2. X. Wang, *Genes Dev.* **15**, 2922–2933 (2001).
3. M. Sato, K. Sato, *Biochim. Biophys. Acta* **1833**, 1979–1984 (2013).
4. B. Levine, Z. Elazar, *Science* **334**, 1069–1070 (2011).
5. Q. Zhou, H. Li, D. Xue, *Cell Res.* **21**, 1662–1669 (2011).
6. S. Al Rawi et al., *Science* **334**, 1144–1147 (2011).
7. M. Sato, K. Sato, *Science* **334**, 1141–1144 (2011).
8. J. Parrish et al., *Nature* **412**, 90–94 (2001).
9. L. Y. Li, X. Luo, X. Wang, *Nature* **412**, 95–99 (2001).
10. J. L. Lin et al., *J. Biol. Chem.* **287**, 7110–7120 (2012).
11. K. Jia, B. Levine, *Adv. Exp. Med. Biol.* **694**, 47–60 (2010).
12. K. Madura, *Trends Biochem. Sci.* **29**, 637–640 (2004).
13. D. C. Wallace, *Environ. Mol. Mutagen.* **51**, 440–450 (2010).
14. J. M. Cummins, *Hum. Reprod.* **15** (suppl. 2), 92–101 (2000).
15. M. S. Sharpley et al., *Cell* **151**, 333–343 (2012).
16. M. Schwartz, J. Vissing, *N. Engl. J. Med.* **347**, 576–580 (2002).
17. N. Lane, *BioEssays* **33**, 860–869 (2011).
18. W. Y. Tsang, B. D. Lemire, *Biochem. Cell Biol.* **80**, 645–654 (2002).
19. G. Ashrafi, T. L. Schwarz, *Cell Death Differ.* **20**, 31–42 (2013).
20. K. Wang, D. J. Klionsky, *Autophagy* **7**, 297–300 (2011).
21. S. Z. DeLuca, P. H. O'Farrell, *Dev. Cell* **22**, 660–668 (2012).
22. C. McDermott-Roe et al., *Nature* **478**, 114–118 (2011).

## ACKNOWLEDGMENTS

We thank T. Blumenthal, R. Poyton, and K. Krauter for comments and H. Zhang for strains and antibodies. Supported by March of Dimes grant 1-FY14-300 and NIH grants GM59083, GM79097, and GM118188 (D.X.) and Research Grants Council of Hong Kong grant AoE/M-05/12 (B.-H.K.).

## SUPPLEMENTARY MATERIALS

www.sciencemag.org/content/353/6297/394/suppl/DC1  
Materials and Methods  
Supplementary Text  
Figs. S1 to S8  
Table S1  
Movie S1  
References (23–37)

14 February 2016; accepted 15 June 2016  
Published online 23 June 2016  
10.1126/science.aaf4777

## CANCER IMMUNOTHERAPY

# Cdk5 disruption attenuates tumor PD-L1 expression and promotes antitumor immunity

R. Dixon Dorand,<sup>1,2</sup> Joseph Nthale,<sup>2,3</sup> Jay T. Myers,<sup>2,3</sup> Deborah S. Barkauskas,<sup>2,3</sup> Stefanie Avril,<sup>1,4</sup> Steven M. Chirieleison,<sup>1</sup> Tej K. Pareek,<sup>2,3</sup> Derek W. Abbott,<sup>1,4</sup> Duncan S. Stearns,<sup>2,3,4</sup> John J. Letterio,<sup>2,3,4</sup> Alex Y. Huang,<sup>1,2,3,4,\*†</sup> Agne Petrosiute<sup>2,3,4,\*†</sup>

Cancers often evade immune surveillance by adopting peripheral tissue-tolerance mechanisms, such as the expression of programmed cell death ligand 1 (PD-L1), the inhibition of which results in potent antitumor immunity. Here, we show that cyclin-dependent kinase 5 (Cdk5), a serine-threonine kinase that is highly active in postmitotic neurons and in many cancers, allows medulloblastoma (MB) to evade immune elimination. Interferon- $\gamma$  (IFN- $\gamma$ )-induced PD-L1 up-regulation on MB requires Cdk5, and disruption of Cdk5 expression in a mouse model of MB results in potent CD4<sup>+</sup> T cell-mediated tumor rejection. Loss of Cdk5 results in persistent expression of the PD-L1 transcriptional repressors, the interferon regulatory factors IRF2 and IRF2BP2, which likely leads to reduced PD-L1 expression on tumors. Our finding highlights a central role for Cdk5 in immune checkpoint regulation by tumor cells.

Cyclin-dependent kinase 5 (Cdk5) is a non-stereotypical Cdk whose activity depends on coactivators, p35 and/or p39. A proline-directed serine-threonine kinase (1), Cdk5 is essential in central nervous system (CNS) development (2, 3). Cdk5 also contributes to angiogenesis, apoptosis, myogenesis, vesicular transport, and senescence in nonneuronal cells, including tumors (4–6), which makes Cdk5 a potential therapeutic target in cancers (7–9). We explored whether Cdk5 plays a role in medulloblastoma (MB), a common malignant pediatric CNS tumor.

MB cell lines and clinical specimens expressed Cdk5, p35, and p39 (Fig. 1A and fig. S1A). Cdk5-specific kinase activity could be abolished in vitro by roscovitine, a nonselective inhibitor against Cdk1, 2, 5, 7, and 9 (fig. S1B) (10). To interrogate Cdk5-specific functions, we disrupted Cdk5 in wild-type murine MB cells (MM1 WT) by short hairpin-mediated RNA interference (MM1 shCdk5) and clustered regularly interspaced short palindromic repeats (CRISPR)-Cas9-targeted mutation (MM1 crCdk5), with nontargeting constructs as controls (MM1 shNS and MM1 crNeg). A reduction in Cdk5 was confirmed at the transcript (fig. S1C) and protein levels (fig. S1D). In vitro, there were no significant differences in cell proliferation among all constructs (fig. S1, E and F) (1).

To assess MB growth in vivo,  $5 \times 10^4$  Cdk5-deficient or control cells were inoculated subcutaneously (s.c.) into the flanks of immunodeficient mice. All mice developed comparable-sized tumors by day 14 (fig. S2, A to C). However, 78 to 50% of C57BL/6 mice injected s.c. with Cdk5-deficient MB cells showed tumor-free survival (TFS) at 19 and 42 days, whereas mice injected with WT and control tumors exhibited 0 and 7% TFS after 19 days, respectively (Fig. 1B and fig. S3A). Mice injected with Cdk5-deficient MB cells developed significantly smaller tumors ( $0.02 \pm 0.04$  g) than mice injected with WT ( $0.91 \pm 0.39$  g) or NS ( $0.51 \pm 0.21$  g) cells (fig. S3B). These data suggest a T cell-dependent rejection mechanism of Cdk5-deficient MM1 cells. This interpretation is supported by the observation that Cdk5 expression inversely correlated with T cell infiltration in human MB (Fig. 1C and fig. S2D).

To identify T cell populations mediating this potent rejection, we depleted CD8<sup>+</sup> T cells, CD4<sup>+</sup> T cells, or both subsets in mice inoculated with MM1 crCdk5 or crNeg cells ( $5 \times 10^4$  s.c.). By day 11, 100% of mice injected with MM1 crNeg and 80% of mice receiving MM1 crCdk5 developed measurable tumors (Fig. 1B), although MM1 crNeg tumors were 8 times the size of MM1 crCdk5 tumors ( $808.8 \pm 382.1$  versus  $101.1 \pm 92.9$  mm<sup>3</sup>) (Fig. 1D). Depletion with CD4-specific ( $\alpha$ CD4) antibody alone or with both  $\alpha$ CD4 and  $\alpha$ CD8 antibodies resulted in 100% MM1 crCdk5 tumor incidence accompanied by rapid tumor growth, whereas CD8 depletion alone yielded 30% TFS, similar to isotype control (Fig. 1D). Among mice receiving isotype antibody, three of eight crCdk5 tumor outgrowths regressed starting on day 17, whereas three of nine crCdk5 tumor outgrowths among mice depleted of CD8<sup>+</sup> T cells regressed starting on day 25; these outgrowths contributed

<sup>1</sup>Department of Pathology, Case Western Reserve University School of Medicine, Cleveland, OH 44106, USA. <sup>2</sup>Division of Pediatric Hematology-Oncology, Department of Pediatrics, Case Western Reserve University School of Medicine, Cleveland, OH 44106, USA. <sup>3</sup>Angie Fowler Adolescent and Young Adult Cancer Institute and University Hospitals Rainbow Babies and Children's Hospital, Cleveland, OH 44106, USA. <sup>4</sup>Case Comprehensive Cancer Center, Case Western Reserve University School of Medicine, Cleveland, OH 44106, USA.

\*These authors contributed equally to this work. †Corresponding author. Email: ahy3@case.edu (A.Y.H.); axp125@case.edu (A.P.)

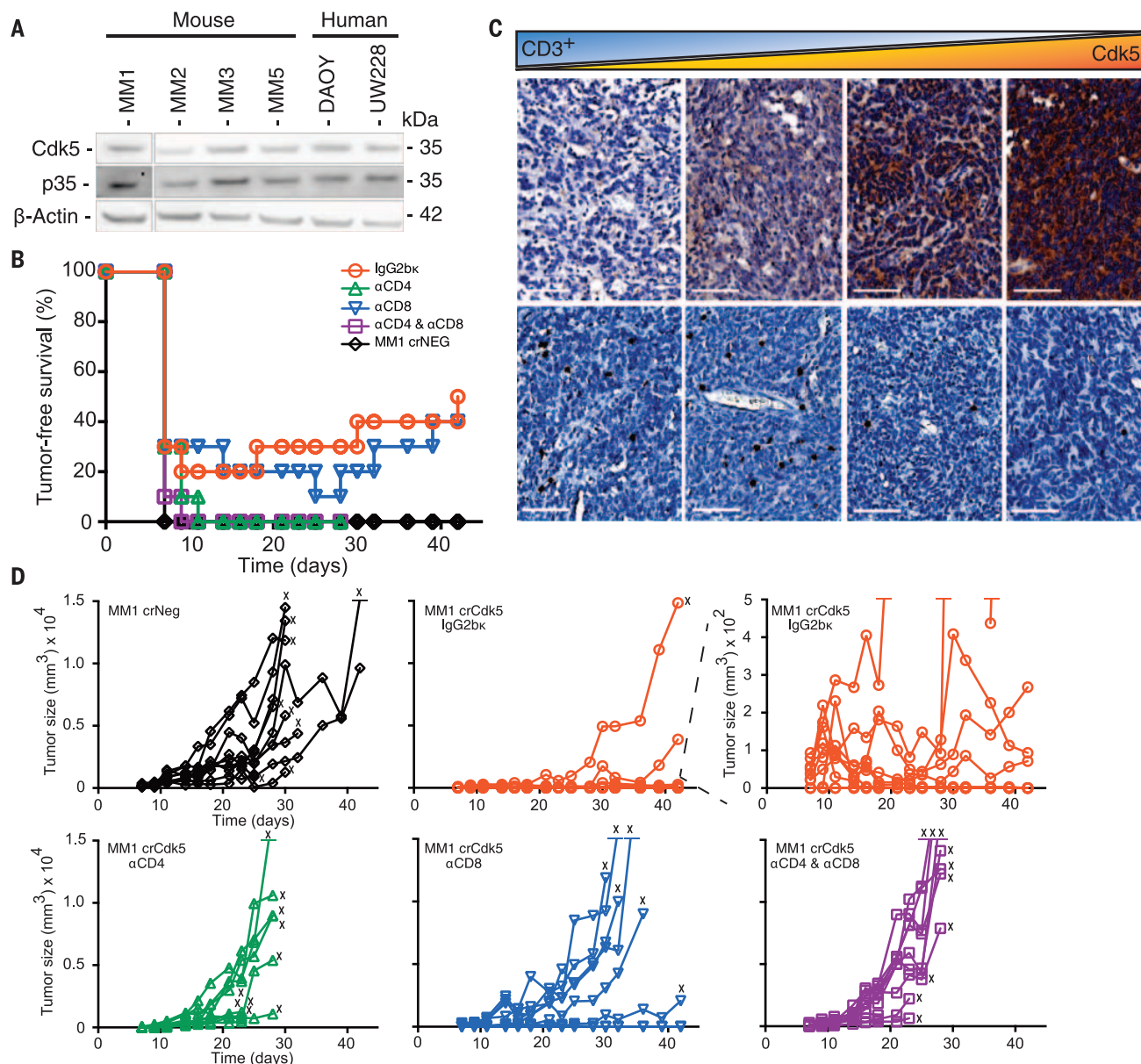


**Fig. 1. Targeted deletion of Cdk5 in MB results in rejection by CD4<sup>+</sup> T cells.** (A) Cdk5 and p35 proteins are expressed in murine and human MB cell lines in vitro. (B) TFS in C57BL/6J mice injected with MM1 crNeg or crCdk5 cells with various depleting antibodies ( $n = 10$  per group). (C) Immunohistochemistry of six clinical MB samples reveals an inverse correlation between tumor Cdk5 expression (top) and CD3<sup>+</sup> T cell infiltration (bottom). Pearson correlation =  $-0.91$  (fig. S2D). Scale bars, 100  $\mu$ m. (D) Tumor-growth kinetics for individual animals in each group from (B). The top right-hand graph shows the center one with an expanded scale. X indicates that an animal was killed because of tumor size or ulceration.

to a total TFS of 50 and 40%, respectively (Fig. 1, B and D). Tumors harvested from MM1 crCdk5-bearing mice remained Cdk5<sup>-</sup> without evidence of Cdk5<sup>+</sup> escape (fig. S4A). Similar results were seen in mice receiving MM1 shCdk5 and shNS inoculations, with a dependency on CD4<sup>+</sup> T cells for tumor rejection (fig. S3C). Cdk5-deficient tumors also grew aggressively in mice deficient in major histocompatibility complex class II (MHC-II) (fig. S3D). Finally, 60 to 75% of mice that rejected Cdk5-deficient tumors remained tumor free after rechallenge with a lethal dose of MM1 WT cells (fig. S3E). Collectively, these studies point to a CD4<sup>+</sup> T cell-dependent rejection of Cdk5-deficient

tumors with robust antitumor immune memory generation.

Interferon- $\gamma$  (IFN- $\gamma$ ) is a major CD4<sup>+</sup> T cell effector cytokine (11) and was abundant in Cdk5-deficient tumor mass (fig. S5A). IFN- $\gamma$  induces p35 (12), which results in enhanced Cdk5 activity (fig. S5B). IFN- $\gamma$  is known to induce PD-L1 (13), whose expression on infiltrating immune cells is evidence of an ongoing intratumoral immune response (14). We examined whether disruption of Cdk5 expression in MB impaired PD-L1 induction in response to IFN- $\gamma$  stimulation. We analyzed human tumor databases and found a cooccurrence of Cdk5 and PD-L1 mRNA expres-

sion in many tumor types (fig. S6). In Cdk5-deficient MM1, we observed a  $37.58 \pm 14.28\%$  reduction in basal PD-L1 mRNA level (Fig. 2A). Note that Cdk5-deficient MM1 cells exhibited a blunted PD-L1 up-regulation in response to IFN- $\gamma$  stimulation in vitro (Fig. 2, A and B, and fig. S4B). Other IFN- $\gamma$ -responsive proteins, such as MHC H-2K<sup>b</sup> and H-2D<sup>b</sup> (fig. S7A), were not significantly affected in the Cdk5-deficient tumors, which indicated that a global disruption of the IFN- $\gamma$  receptor (IFNGR) signaling was not responsible for failed PD-L1 up-regulation or enhanced immune sensitivity. Disrupting Cdk5 in rhabdomyosarcoma also led to a blunted

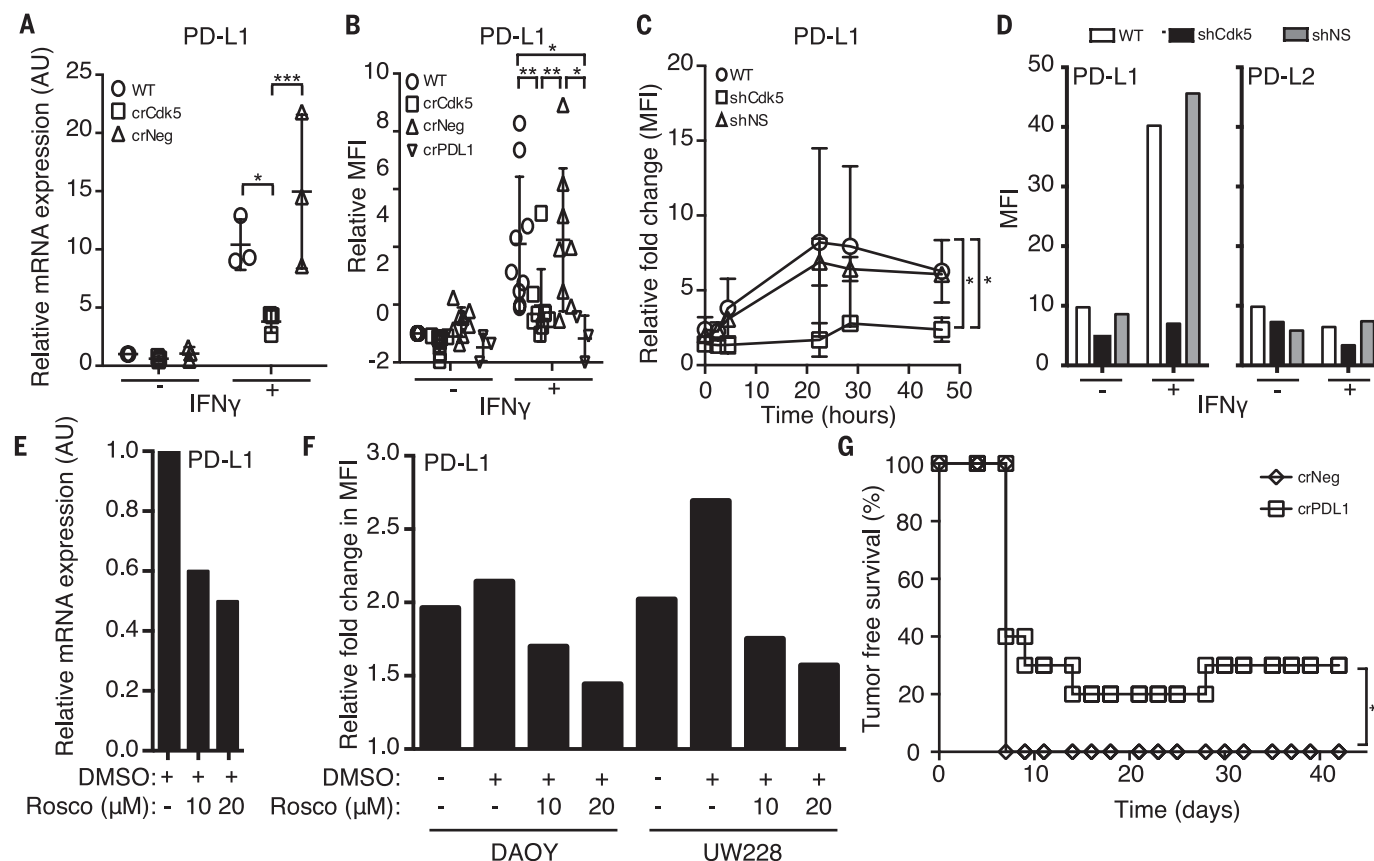


**Fig. 2. Disruption of either Cdk5 gene expression or Cdk5 activity suppresses PD-L1 expression that cannot be overcome with IFN- $\gamma$  stimulation in both human and murine MBs.** (A) In vitro mRNA expression in arbitrary units (AU) of *PD-L1* by MM1 WT, crCdk5, and crNeg cells with or without 24 hours of IFN- $\gamma$  stimulation. Values represent the average of three biological replicates  $\pm$  SD. (B) In vitro PD-L1 surface staining of MM1 WT, crCdk5, crNeg, and crPDL1 cells with or without 24 hours of IFN- $\gamma$  stimulation. Values represent the average mean fluorescence intensity (MFI)  $\pm$  SD compared with unstimulated MM1 WT cells over seven or eight replicates. (C) Fold change of surface PD-L1 expression in MM1 WT, shCdk5, and shNS cells over

the course of 48 hours of IFN- $\gamma$  stimulation. (D) MFI of PD-L1 and PD-L2 expressed in MM1 WT, shCdk5, and shNS cells. (E) *PD-L1* mRNA expression in MM1 WT cells when treated with roscovitine and stimulated with IFN- $\gamma$  for 24 hours. AU relative to untreated. DMSO, dimethyl sulfoxide. (F) DAOY and UW228 human MB lines treated with roscovitine and stimulated with IFN- $\gamma$  for 24 hours. MFI relative to untreated samples. (G) TFS of MM1 crNeg and crPDL1 injected mice over 36 days ( $n = 10$  mice per group). \* $P < 0.05$ ; \*\* $P < 0.01$ ; \*\*\* $P < 0.001$ . Significance was determined by two-way ANOVA with Bonferroni posttest (A) and (B), Student's  $t$  test (C), or log-rank test (G). Representative experiments are shown in (D) and (E).

IFN- $\gamma$ -induced PD-L1 up-regulation (fig. S4, C to E), which indicated that the link between Cdk5 and PD-L1 regulation by IFN- $\gamma$  is not MB-specific. Twenty-four hours after IFN- $\gamma$  exposure, surface PD-L1 expression reached a peak of 8.2- and 6.8-fold above baseline in WT and NS cells, respectively (Fig. 2C), whereas Cdk5-deficient cells only up-regulated PD-L1 2.8-fold, so it reached a peak level similar to the basal levels in unstimulated WT and NS controls. The blunted response to IFN- $\gamma$  is specific for PD-L1 but not PD-L2 (Fig. 2D). To further corroborate the link between Cdk5 and PD-L1 synthesis, we treated MM1 WT cells with roscovitine and observed a dose-dependent decrease in PD-L1 transcripts (Fig. 2E). In vitro treatment of human MB with roscovitine also diminished surface PD-L1 up-regulation with IFN- $\gamma$  in a dose-dependent manner (Fig. 2F). Finally, to establish a functional link between PD-L1 and in vivo rejection of Cdk5-deficient MM1, we disrupted the PD-L1 gene (*CD274*) in MM1 cells (MM1 crPDL1). Similar to MM1 crCdk5 experiments, 30% of mice

inoculated with MM1 crPDL1 remained tumor-free for more than 4 weeks (Figs. 2G and 1B).

Next, we interrogated the IFNGR signaling pathway. Western blot analysis of various MM1 cells failed to show differences, after IFN- $\gamma$  exposure, in STAT1, STAT2, or STAT3 (members of the family of signal transducers and activators of transcription) (Fig. 3A and fig. S7B), in agreement with the robust MHC class I induction in Cdk5-deficient MM1 cells (fig. S7A). To further dissect this STAT1-independent signaling, we examined interferon regulatory factor-1 (IRF1) and interferon regulatory factor-2 (IRF2), which are implicated as positive and negative regulators of PD-L1 transcription, respectively (13, 15). IRF1 protein was rapidly induced by IFN- $\gamma$  and remained elevated for up to 48 hours regardless of Cdk5 expression (Fig. 3A and fig. S7C). We observed a rapid loss of the PD-L1 transcription repressor, IRF2, in WT and crNeg cells. In contrast, IRF2 and its corepressor IRF2BP2 (16) were elevated at baseline in Cdk5-deficient cells and persisted for up to 48 hours after IFN- $\gamma$  exposure (Fig. 3A and fig. S7C). This protein ex-

pression difference cannot be accounted for at the transcriptional level (fig. S7D). Phosphoproteomic analysis identified 77 distinct phosphopeptides in the shCdk5 versus WT or shNS screen (tables S1 and S2), and 798 phosphopeptides in the crCdk5 versus WT or crNeg screen (tables S3 and S4). Between these two data sets, 22 common proteins were differentially phosphorylated in Cdk5-deficient cells, with IRF2BP2 among the highest phosphorylated peptide species (Fig. 3B).

Finally, we introduced Cdk5-deficient MM1 cells orthotopically into C57BL/6 mice. Gross inspection revealed a 50% tumor incidence in mice injected with Cdk5-deficient MM1, mirroring s.c. tumors. In contrast, 100% of mice injected with WT or NS MM1 cells developed gross brain tumors by day 14 (fig. S8A). Intracranial (i.c.) Cdk5-deficient tumor outgrowth remained devoid of Cdk5 expression without the emergence of a Cdk5<sup>+</sup> escape variant (fig. S8B). Histological analysis showed increased accumulation of IBA1<sup>+</sup> cells, which marks microglia and infiltrating monocytes, and PD-L1<sup>+</sup>



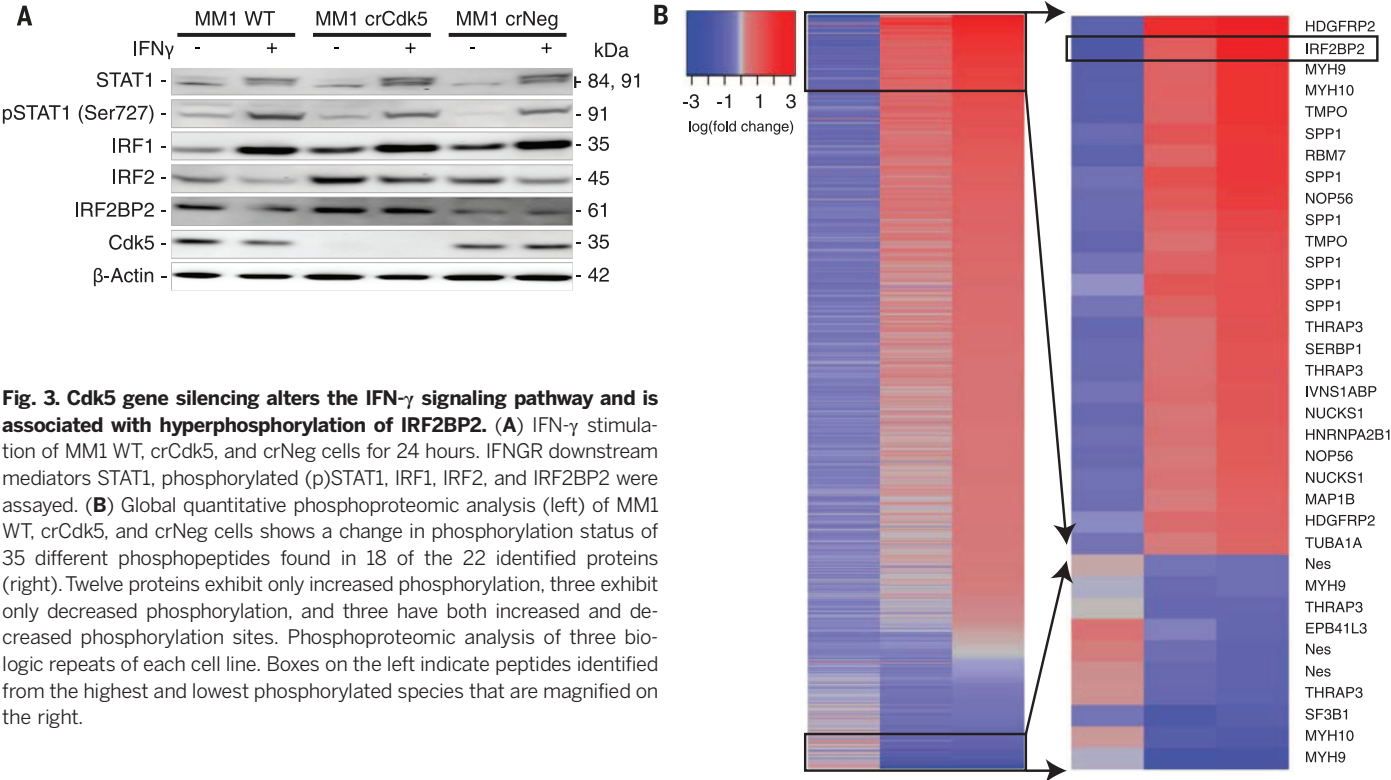


**Fig. 3. Cdk5 gene silencing alters the IFN- $\gamma$  signaling pathway and is associated with hyperphosphorylation of IRF2BP2.** (A) IFN- $\gamma$  stimulation of MM1 WT, crCdk5, and crNeg cells for 24 hours. IFN $\gamma$  downstream mediators STAT1, phosphorylated (p)STAT1, IRF1, IRF2, and IRF2BP2 were assayed. (B) Global quantitative phosphoproteomic analysis (left) of MM1 WT, crCdk5, and crNeg cells shows a change in phosphorylation status of 35 different phosphopeptides found in 18 of the 22 identified proteins (right). Twelve proteins exhibit only increased phosphorylation, three exhibit only decreased phosphorylation, and three have both increased and decreased phosphorylation sites. Phosphoproteomic analysis of three biologic repeats of each cell line. Boxes on the left indicate peptides identified from the highest and lowest phosphorylated species that are magnified on the right.

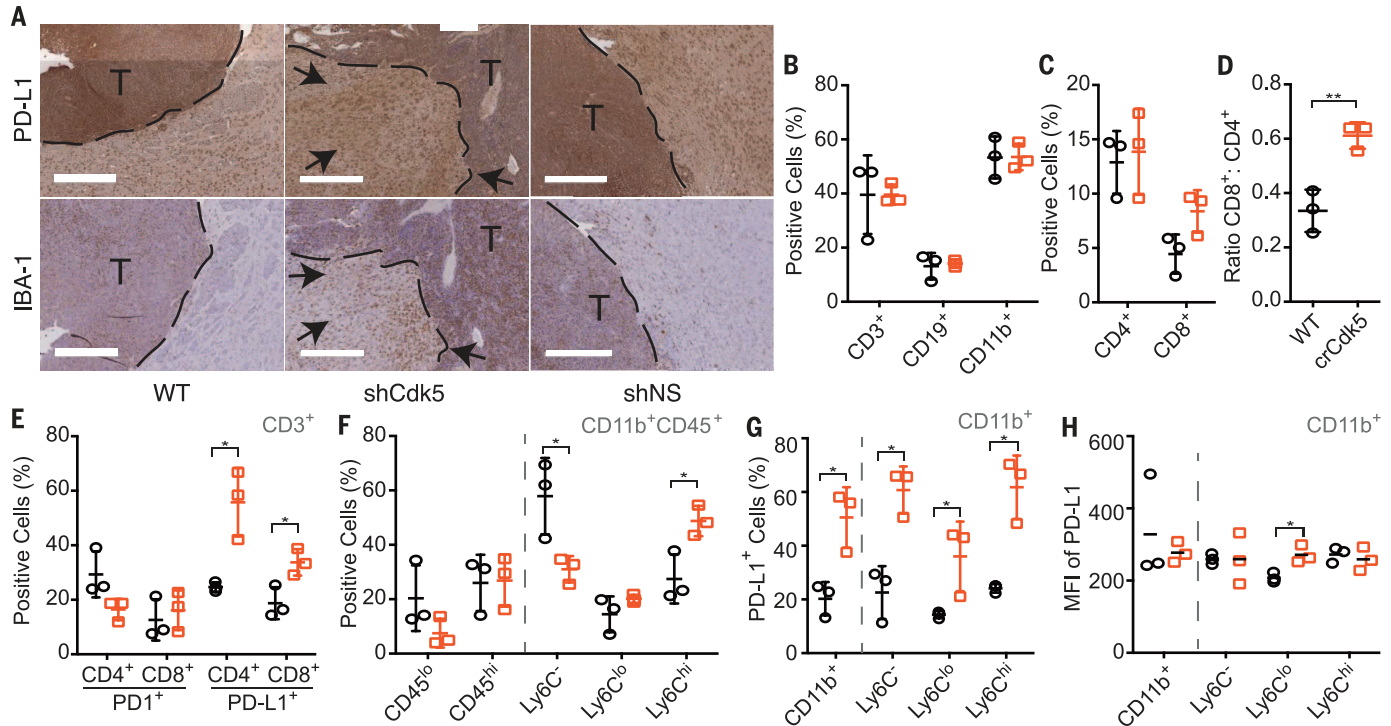


**Fig. 4. Orthotopic Cdk5-deficient tumors exhibit increased PD-L1 staining, CD4 $^{+}$  tumor-infiltrating lymphocytes (TILs), and accumulating infiltrates of CD11b $^{+}$  populations.** (A) Tumors extracted 14 days postinoculation from MM1 WT, shCdk5, or shNS mice stained for PD-L1 expression. Dashed line represents margin between tumor (T) and stroma. Black arrows point to increased PD-L1 $^{+}$  and IBA-1 $^{+}$  cells in the tumor stroma. Scale bars, 400  $\mu$ m. (B and C) Fluorescence-activated cell sorting (FACS) analysis of MM1 WT (black circle) and MM1 crCdk5 (orange square) tumor infiltrate by percentage of cell type. (D) Ratio of total CD8 $^{+}$ :CD4 $^{+}$  cell infiltrate. (E) FACS analysis of the percentage of PD-L1 $^{+}$  or PD-L1 $^{+}$  cells in the CD4 $^{+}$  or CD8 $^{+}$  populations. (F) FACS analysis of the percentage of myeloid cells in tumor infiltrate based on differential CD45 staining (left) or Ly6C staining among CD11b $^{+}$ CD45 $^{+}$  cells (right). (G) Percent of total CD11b $^{+}$  population (left) and subpopulations (right) present in tumor infiltrate that express PD-L1. (H) MFI of PD-L1 expression among CD11b $^{+}$  total population (left) and subpopulations (right). (B), (C), (D), (E), (F), and (G) were graphed as means  $\pm$  SD. (H) was graphed as individual MFI with mean indicated.  $n = 9$  per group. Each data point represents pooled samples from three mice. \* $P < 0.05$ ; \*\* $P < 0.01$ . Significance was determined using the Student's  $t$  test.

staining in the Cdk5-deficient MM1 tumor margin and surrounding stroma (Fig. 4A). Immune cell composition analysis showed a modest increase in CD3<sup>+</sup> T cells, similar to that shown by immunohistochemical data (Fig. 1C and fig. S8, C and D). However, the percentages of CD3<sup>+</sup> cells were equivalent in crCdk5 and WT tumor samples by flow cytometry (Fig. 4B). Cdk5-deficient tumors elicited an increased ratio of CD8<sup>+</sup> to CD4<sup>+</sup> T cell infiltrate, lower PD-1 expression in CD4<sup>+</sup> T cells, and higher PD-L1 expression in both T cell subsets (Fig. 4, C to E). Although CD8<sup>+</sup> T cells are not the primary antitumor effector cells in this model, their increased recruitment likely reflects an overall inflammatory tumor milieu as evidenced by increased PD-L1 expression and overall tissue IFN- $\gamma$  levels (Fig. 1B and figs. S3C, S5A, and S9, A to E). The myeloid infiltrate in i.c. tumors shifted from a Ly6C<sup>+</sup> to a Ly6C<sup>hi</sup> population with an increased percentage of PD-L1<sup>+</sup> cells in bulk CD11b<sup>+</sup> cells and in each Ly6C subset (Fig. 4, F to H), accompanied by a decrease in the percentage of microglia (CD11b<sup>+</sup>CD45<sup>lo</sup>) (Fig. 4F). The Ly6C<sup>lo</sup> subset expressed a higher density of surface PD-L1 in the Cdk5-deficient tumors (Fig. 4H). Again, this finding was recapitulated in s.c. tumors, which showed a significant increase in the percentage of PD-L1<sup>+</sup> immune cells, with a trend toward increased density of PD-L1 staining in the crCdk5 tumor microenvironment (fig. S9, F to I). The observed increase in PD-L1<sup>+</sup> populations and staining density aligns with histologic analyses (Fig. 4A and fig. S9B), which suggests a state of global immune activation in response to ongoing IFN- $\gamma$  stimulation. This finding is in good agreement with reports showing increased PD-L1<sup>+</sup> immune cells in MB stroma undergoing active immune checkpoint blockade (17).

Here, we showed that Cdk5 disruption sensitizes MB to CD4<sup>+</sup> T cell-dependent rejection via posttranslational modification of IRF2BP2, which increases IRF2 and IRF2BP2 abundance and sustains PD-L1 transcriptional repression after IFN- $\gamma$  stimulation. Downstream IFN- $\gamma$  signaling induces interferon-stimulated genes, including *IRF1* (18), which activates secondary-response genes, including *PD-L1* (13, 19, 20). IRF2 acts as a repressor that competes with IRF1 for binding to the same promoter element (15). Constitutively

present, IRF2 is up-regulated in response to either type I IFNs or IRF1 (15, 20) and provides a negative-feedback loop by binding to its own promoter to block transcription (15). The prolonged half-life of IRF2 (8 hours) relative to IRF1 (0.5 hours) provides a mechanism for IRF2 antagonism (20). IRF2BP2 was recently identified as a corepressor with IRF2 (16), and low IRF2BP2 expression was correlated with high PD-L1 expression in breast cancer (21). Our data provide a direct link between disruption of Cdk5 activity and IRF2BP2 hyperphosphorylation at sites that are distinct from previously described sites that affect nuclear localization, vascular endothelial growth factor A, or MHC-I expression (22–24), which suggests that Cdk5 either directly or indirectly inhibits other kinase(s) that phosphorylate IRF2BP2 (fig. S10).

PD-L1 and PD-1 play a critical role in tumor immune evasion, with ~30% of tumors responding to immune checkpoint blockade (25, 26). High Cdk5 expression correlates with worse clinical outcome in multiple cancers (fig. S11). In our studies, both Cdk5- and PD-L1-deficient MB cells exhibit similar TFS (Figs. 1B and 2G). More CD4<sup>+</sup> T cells with lower PD-1 expression were found in the Cdk5-deficient CNS tumors, whereas CD11b<sup>+</sup> cells accumulate in larger quantities with higher PD-L1<sup>+</sup> expression (Fig. 4, C to G). Myeloid PD-L1 up-regulation may be a response to overall increased IFN- $\gamma$  (13, 27). Alternatively, these cells may play a distinct role modulating infiltrating T cell function, which are present in most human MB specimens (28). Last, as Cdk5 directly phosphorylates MYC on Ser<sup>62</sup> (29), it remains to be determined whether Cdk5 plays a role in MYC-regulated PD-L1 expression (30).

## REFERENCES AND NOTES

- R. Dhavan, L. H. Tsai, *Nat. Rev. Mol. Cell Biol.* **2**, 749–759 (2001).
- T. Ohshima et al., *Proc. Natl. Acad. Sci. U.S.A.* **93**, 11173–11178 (1996).
- E. Utreras, A. Futatsugi, T. K. Pareek, A. B. Kulkarni, *Drug Discov. Today Ther. Strateg.* **6**, 105–111 (2009).
- E. Contreras-Vallejos, E. Utreras, C. Gonzalez-Billault, *Cell. Signal.* **24**, 44–52 (2012).
- A. Arif, *Biochem. Pharmacol.* **84**, 985–993 (2012).
- T. K. Pareek et al., *J. Exp. Med.* **207**, 2507–2519 (2010).
- F. N. Hsu et al., *J. Biol. Chem.* **286**, 33141–33149 (2011).
- G. Feldmann et al., *Cancer Res.* **70**, 4460–4469 (2010).
- R. Liu et al., *Proc. Natl. Acad. Sci. U.S.A.* **105**, 7570–7575 (2008).
- H. S. Khalil, V. Mitev, T. Vlaykova, L. Cavicchi, N. Zhelev, *J. Biotechnol.* **202**, 40–49 (2015).
- H. J. Kim, H. Cantor, *Cancer Immunol. Res.* **2**, 91–98 (2014).
- J. H. Song et al., *J. Biol. Chem.* **280**, 12896–12901 (2005).
- S. J. Lee et al., *FEBS Lett.* **580**, 755–762 (2006).
- J. M. Taube et al., *Sci. Transl. Med.* **4**, 27ra37 (2012).
- H. Harada et al., *Cell* **58**, 729–739 (1989).
- K. S. Childs, S. Goodbourn, *Nucleic Acids Res.* **31**, 3016–3026 (2003).
- C. D. Pham et al., *Clin. Cancer Res.* **22**, 582–595 (2016).
- L. C. Platanias, *Nat. Rev. Immunol.* **5**, 375–386 (2005).
- S. Yao et al., *Mucosal Immunol.* **8**, 746–759 (2015).
- T. Taniguchi, A. Takaoka, *Nat. Rev. Mol. Cell Biol.* **2**, 378–386 (2001).
- H. Soliman, F. Khalil, S. Antonia, *PLOS ONE* **9**, e88557 (2014).
- A. C. Teng et al., *PLOS ONE* **6**, e24100 (2011).
- A. C. Teng et al., *FASEB J.* **24**, 4825–4834 (2010).
- K. W. Jarosinski, P. T. Massa, *J. Neuroimmunol.* **122**, 74–84 (2002).
- D. M. Pardoll, *Nat. Rev. Cancer* **12**, 252–264 (2012).
- W. Zou, L. Chen, *Nat. Rev. Immunol.* **8**, 467–477 (2008).
- J. Liu et al., *Blood* **110**, 296–304 (2007).
- V. S. Salsman et al., *PLOS ONE* **6**, e20267 (2011).
- H. R. Seo, J. Kim, S. Bae, J. W. Soh, Y. S. Lee, *J. Biol. Chem.* **283**, 15601–15610 (2008).
- S. C. Casey et al., *Science* **352**, 227–231 (2016).

## ACKNOWLEDGMENTS

We thank F. Scrimieri, G. Valdivieso, A. Awadallah, A. Kresak, D. Schlatter, and the Case Western Reserve University Center for Proteomics for technical assistance; M. Couce for constructing human MB tissue microarray; and M. Chieppa, D. Askew, and B. Benson for careful review of the manuscript. The data reported in this manuscript are tabulated in the main paper and in the supplementary materials. This work was supported by NIH F31CA196265 (R.D.D.), NIH T32GM007250 (R.D.D. and S.M.C.), NIH T32AI089474 (S.M.C.), NIH R01GM086550 (D.W.A.), NIH R01CA154656 (A.Y.H.), NIH R21CA181875 (A.Y.H. and J.J.L.), NIH R01HL111682 (A.Y.H. and J.J.L.), NIH P30CA043703 (A.Y.H. and A.P.), Wolstein Research Scholarship (R.D.D.), St. Baldrick's Foundation (A.P., J.J.L., and A.Y.H.), Hyundai "Hope-on-Wheels" Program (A.P., D.S.S., and A.Y.H.), Marc Joseph Fund (A.Y.H.), Alex's Lemonade Stand Foundation (A.P. and A.Y.H.), the Angie Fowler Adolescent and Young Adult Cancer Research Initiative at the Case Comprehensive Cancer Center (A.P., J.J.L., D.S.S., S.A., and A.Y.H.), and Theresa G. and Stuart F. Kline Family Foundation in Pediatric Oncology (A.Y.H.). This work was supported by the Clinical and Translational Science Collaborative of Cleveland UL1TR000439 (A.P.), and KL2TR000440 (S.A.) from the National Center for Advancing Translational Sciences (NCATS) component of the NIH. Authors declare no competing financial interests. All phosphoproteomics data are available in the supplementary materials.

## SUPPLEMENTARY MATERIALS

www.sciencemag.org/content/353/6297/399/suppl/DC1  
Materials and Methods  
Figs. S1 to S11  
Tables S1 to S4  
Reference (31)

9 December 2015; accepted 31 May 2016  
10.1126/science.aae0477



# Cdk5 disruption attenuates tumor PD-L1 expression and promotes antitumor immunity

R. Dixon Dorand, Joseph Nthale, Jay T. Myers, Deborah S. Barkauskas, Stefanie Avril, Steven M. Chirieleison, Tej K. Pareek, Derek W. Abbott, Duncan S. Stearns, John J. Letterio, Alex Y. Huang and Agne Petrosiute (July 21, 2016)  
*Science* **353** (6297), 399-403. [doi: 10.1126/science.aae0477]

Editor's Summary

## Cyclin suppresses antitumor immunity

Despite the dramatic success of cancer immunotherapy, many types of cancer do not respond. Understanding why could help us to find ways to enhance the overall responsiveness of tumors to immunotherapies. Dorand *et al.* report that cyclin-dependent kinase 5 (Cdk5), an enzyme that is highly expressed by neurons in many brain cancers, may dampen the ability of T cells to reject tumors. In a mouse model of medulloblastoma, if tumors were Cdk5 deficient, T cells were able to remove them. This heightened antitumor immunity correlated with reduced expression of the inhibitory molecule programmed cell death ligand 1 (PD-L1), a target of current cancer immunotherapies.

*Science*, this issue p. 399

---

This copy is for your personal, non-commercial use only.

---

### Article Tools

Visit the online version of this article to access the personalization and article tools:  
<http://science.sciencemag.org/content/353/6297/399>

### Permissions

Obtain information about reproducing this article:  
<http://www.sciencemag.org/about/permissions.dtl>

*Science* (print ISSN 0036-8075; online ISSN 1095-9203) is published weekly, except the last week in December, by the American Association for the Advancement of Science, 1200 New York Avenue NW, Washington, DC 20005. Copyright 2016 by the American Association for the Advancement of Science; all rights reserved. The title *Science* is a registered trademark of AAAS.